Physics in Medicine & Biology

IPEM Institute of Physics and Engineering in Medicine

ACCEPTED MANUSCRIPT • OPEN ACCESS

Robust optimization and assessment of dynamic trajectory and mixed-beam arc radiotherapy: apreliminary study

To cite this article before publication: Jenny Bertholet *et al* 2024 *Phys. Med. Biol.* in press https://doi.org/10.1088/1361-6560/ad6950

Robust optimization and assessment of dynamic trajectory and mixed-beam arc radiotherapy: a preliminary study

Jenny Bertholet[1], Gian Guyer, Silvan Mueller, Hannes A Loebner, Werner Volken, Daniel M Aebersold, Peter Manser, Michael K Fix

Division of Medical Radiation Physics and Department of Radiation Oncology, Inselspital, Bern University Hospital, and University of Bern, 3010 Bern, Switzerland

[1]Corresponding author: Jenny Bertholet, jenny.bertholet@insel.ch

Abstract

Objective. Dynamic trajectory radiotherapy (DTRT) and dynamic mixed-beam arc therapy (DYMBARC) exploit non-coplanarity and, for DYMBARC, simultaneously optimized photon and electron beams. Margin concepts to account for set-up uncertainties during delivery are ill-defined for electron fields. We develop robust optimization for DTRT&DYMBARC and compare dosimetric plan quality and robustness for both techniques and both optimization strategies for four cases.

Approach. Cases for different treatment sites and clinical target volume (CTV) to planning target volume (PTV) margins, m, were investigated. Dynamic gantry-table-collimator photon paths were optimized to minimize PTV/organ-at-risk (OAR) overlap in beam's-eye-view and minimize potential photon multileaf collimator (MLC) travel. For DYMBARC plans, non-isocentric partial electron arcs or static fields with shortened source-to-surface distance (80 cm) were added. Direct aperture optimization (DAO) was used to simultaneously optimize MLC-based intensity modulation for both photon and electron beams yielding deliverable PTV-based DTRT&DYMBARC plans. Robust-optimized plans used the same paths/arcs/fields. DAO with stochastic programming was used for set-up uncertainties with equal weights in all translational directions and magnitude δ such that $m = 0.7\delta$. Robust analysis considered random errors in all directions with or without an additional systematic error in the worst 3D direction for the adjacent OARs.

Main results. Electron contribution was 7%-41% of target dose depending on the case and optimization strategy for DYMBARC. All techniques achieved similar CTV coverage in the nominal (no error) scenario. OAR sparing was overall better in the DYMBARC plans than in the DTRT plans and DYMBARC plans were generally more robust to the considered uncertainties. OAR sparing was better in the PTV-based than in robust-optimized plans for OARs abutting or overlapping with the target volume, but more affected by uncertainties.

Significance. Better plan robustness can be achieved with robust optimization than with margins. Combining electron arcs/fields with non-coplanar photon trajectories further improves robustness and OAR sparing.

Introduction

Advanced radiotherapy treatment techniques like dynamic trajectory radiotherapy (DTRT) and mixed-beam dynamic trajectory radiotherapy (DYMBER) can dose to the organs-at-risk (OARs) compared to state-of-the-art techniques by exploiting multiple degrees of freedom of conventional C-arm linear accelerators (linacs) (Fix *et al* 2018, Mueller *et al* 2018). DTRT exploits dynamic table and collimator rotation to deliver intensity-modulated radiation during continuous gantry rotation (Fix *et al* 2018, Bertholet *et al* 2022, Smyth *et al* 2013, Yang *et al* 2011, Langhans *et al* 2018). In DYMBER, static electron fields are additionally considered to reduce the dose at depth for target with a superficial component (Mueller *et al* 2018). The photon multi-leaf collimator (MLC) is used for intensity modulation of both the photon trajectories and the electron fields, and non-isocentric geometry can maintain a shortened source-to-surface distance (SSD) and reduce lateral in-air scatter for the electron fields (Mueller *et al* 2018). Both photon trajectories and electron fields are simultaneously optimized during direct aperture optimization (DAO) so that the relative contribution of each particle type and energy is optimized. We have previously reported on DTRT and DYMBER using static step-and-shoot electron fields (Mueller *et al* 2018, Fix *et al* 2018). More recently, Guyer et al (2023a) combined photon and electron arcs in a non-isocentric but coplanar geometry. Here, we consider dynamic mixed beam arc therapy (DYMBARC) as a generalization of the DYMBER technique. In this work, DYMBARC combines non-coplanar DTRT photon trajectories with non-isocentric coplanar electron arcs.

In addition to dosimetric quality, robustness to clinically relevant delivery uncertainties is an essential aspect of treatment plan quality which must be considered prior to the implementation of new techniques (Hernandez *et al* 2020). Patient set-up uncertainties are conventionally handled by extending the clinical target volume (CTV) with a planning target volume (PTV) margin. Margin concepts based on uncertainty budgets were derived for intensity-modulated radiotherapy (IMRT) and volumetric modulated arc therapy (VMAT) (Stroom and Heijmen 2002, Stroom *et al* 1999, van Herk 2004) with planning at risk volumes (PRV) commonly used to avoid overdosage of serial OARs. However, for electron beams, the depths of the different isodoses are unaffected by errors in the beam direction. Yet, in the direction perpendicular to the beam, the penumbra breadth varies rapidly with depth and energy. Hence, standard margin concepts are ill-defined for electron fields where margins should be three times larger in the direction perpendicular to the beam axis than in the direction of the beam axis (Thomas 2006). This makes the margin concept unsuited for mixed-beam techniques and/or electron arcs. Furthermore, in practice, margins are often manipulated (cropped at the skin to allow for build-up of the photon dose or at the interface with serial OARs to avoid overdosing them) which may compromise the robustness of target coverage. The unsuitability of the margin concept remains an important barrier to the potential clinical implementation of mixed photon-electron treatment techniques.

Robust optimization is an alternative to margins whereby uncertainty scenarios are considered directly during optimization (Unkelbach *et al* 2018). This approach is frequently used in proton therapy, where margin concepts are also ill-defined and do not address range uncertainties (Korevaar *et al* 2019). Robust optimization has been used for mixed photon-electron techniques with fixed beam directions (Renaud *et al* 2019, Heath *et al* 2021) but not for dynamic techniques that include electron arcs with variation in beam directions.

The purpose of this study is to develop a treatment planning process for the robust optimization and assessment of DTRT and DYMBARC plans. We investigated dosimetric plan quality, relative photon/electron contribution for DYMBARC, and the robustness of PTV-based and robust-optimized DTRT and DYMBARC plans to random and systematic set-up uncertainties for four treatment sites.

Methods

The treatment planning and evaluation process is illustrated in the red box of Figure 1. This takes place within an in-house software suite, interfacing with the Eclipse treatment planning system (Research version, Varian, a Siemens Healthineers company) (blue box) via the Eclipse Scripting Application Programming Interface (ESAPI) to provide input to the in-house software (yellow arrows) or enable visualization of the paths or dose distribution (green arrows).

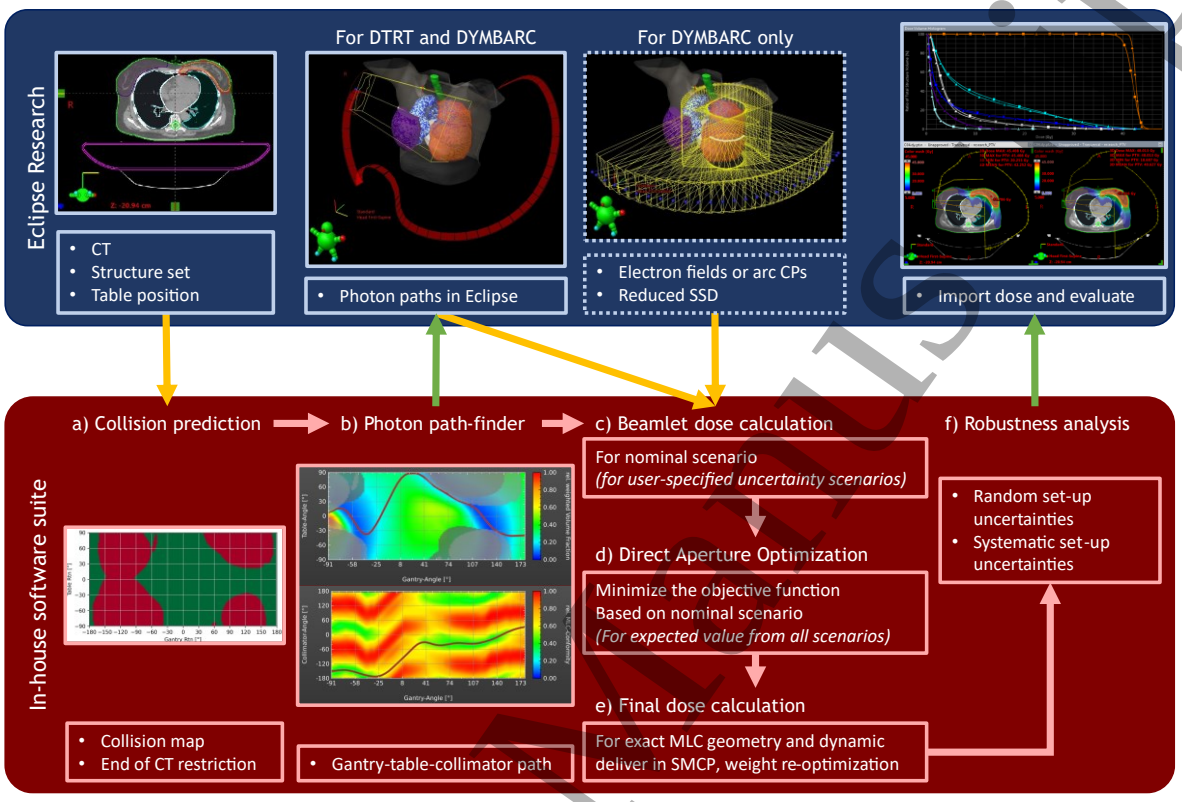

Figure 1. Treatment planning and evaluation process (red box). The Eclipse treatment planning system (blue rectangle) interfaces with in-house software via the research ESAPI, to provide input (yellow arrows) or enable visualization of path and dose distributions (green arrows). Each step of the process is described in detail in the text. Elements in italics and in parentheses apply only to the robust optimization workflow.

a) The CT, structure set and estimated table positions are exported from a research version of Eclipse into an in-house collision prediction tool (Guyer *et al* 2023b) to detect beam directions that may lead to collision. Beam direction leading to beam entry through the end of the CT stack are also excluded.

b) Gantry-table-collimator photon paths are determined to minimize fractional PTV/OAR overlap in beam's-eye-view and minimize the range of possible leaf-travel. Photon paths are split into control points with a 5° gantry resolution and imported in Eclipse (Fix *et al* 2018).
For DYMBARC plans, either electron fields or a set of control points (every 5° gantry angle), to define electron arcs, are set up with a shortened SSD of 80 cm using a script in Eclipse (Guyer *et al* 2023a).

c) Beamlet dose calculation for the fields and control points is started from Eclipse and performed within the Swiss Monte Carlo Plan (SMCP) framework with pre-simulated phase-spaces located at the treatment head exit plane as a source (Fix *et al* 2007, Mueller *et al* 2023). If robust optimization is used, beamlet doses are calculated for all user-specified uncertainty scenarios in addition to the nominal (i.e. no uncertainty) scenario (Heath *et al* 2021).

d) Intensity modulation for photon paths and electron fields/arcs, are optimized simultaneously using a DAO algorithm (Mueller *et al* 2022, Guyer *et al* 2022). If robust optimization is used, each DAO optimization step considers the expected value of the objective function calculated for the nominal scenario and the considered uncertainty scenarios with equal weights using stochastic programming (Heath *et al* 2021).
For DYMBARC plans, a first optimization is performed considering the photon paths and all electron energies for the chosen field/arc set-up. Then the two electron energies that contribute the most to target dose are selected and the other ones are removed for the creation of the final plan (Guyer *et al* 2023a).

e) The final dose calculation is performed in the SMCP framework (Fix *et al* 2007, Manser *et al* 2019) considering the exact MLC geometry and the dynamic movement of the different machine components. The electron beam source model consists of a primary and jaw source (Henzen *et al* 2014, Fix *et al* 2023). Electron dose is calculated using the Macro Monte Carlo algorithm (Neuenschwander *et al* 1995, Fix *et al* 2013). The photon source is a pre-simulated phase-space located at the plane above the secondary collimator jaws. Photon dose is calculated using the Voxel Monte Carlo (VMC++) algorithm (Kawrakow and Fippel 2000). Subsequently, the monitor units' weights are reoptimized to mitigate differences between the beamlet-based and the final dose calculation.

f) PTV-based and robust-optimized plans are all subject to robustness analysis using a Monte Carlo robustness calculation and evaluation tool, where multiple random or systematic uncertainty scenarios can be considered and combined (Loebner *et al* 2022).

DTRT and DYMBARC plans are created for four cases described in table 1. The same optimization objectives were used for both PTV-based plans (objective types were upper and lower dose-volume objectives, generalized equivalent uniform dose objectives, and normal tissue objectives (Mueller *et al* 2022)). They were determined iteratively such CTV coverage was similar for both techniques and all OARs contributed to the cost function for both plans. For the robust-optimized plans, optimization objectives for PTV and PRVs were applied to the CTV and the corresponding OARs, respectively. In principle, for robust-optimized plans, the paths would be calculated using a CTV/OAR overlap map (step b). However, in this study, the same photon paths are used as for the PTV-based plan, since only minimal differences would be expected.

Robustness analysis is performed for a random translational set-up error scenario, which also includes the combination of errors in multiple directions. Here σ, such that $m = 0.7\sigma$ is the standard deviation of the gaussian distribution used to sample a set-up error for each fraction (Loebner *et al* 2022), where m is the CTV-PTV margin in the PTV-based optimization. An additional scenario with combined random errors and systematic set-up error (of magnitude 0.5σ) in the direction (in 3D) that pushes nearby OARs into the high dose region is also considered as a possible worst-case scenario for OAR sparing (table 1).

Of note, the clinical plan of the head and neck case included a bolus and the PTV was cropped at the skin where there was no bolus. However, in this study, all the plans were without bolus. This is motivated by the hypothesis that a bolus may not be needed to obtain target coverage for superficial targets when using non-coplanar beam directions and/or electron fields.

PTV-based and robust-optimized DTRT and DYMBARC plans are compared based on relative photon/electron contribution to the target dose in the DYMBARC plans and on dosimetric end-points for the nominal scenario, random errors only, and the combined random and systematic error scenarios.

Table 1: description of the cases, optimization parameters, and robustness analysis parameters.

Case	Brain	Head and neck[3]	Pelvis	Breast
Optimization parameters				
Prescription[1]	30 x 2.00 Gy	25 x 2.00 Gy	29 x 1.80 Gy	16 x 2.65 Gy
CTV-PTV margin, m	m = 3.0 mm	m = 3.0 mm	m = 2.0 mm	m = 5.0 mm
Margin manipulation	Cropped at brainstem PRV and right optic nerve PRV	Cropped at the skin[3]	None	Cropped at the skin
Shift, δ, for robust optimization[2]	δ = 4.0 mm	δ = 4.0 mm	δ = 3.0 mm	δ = 7.0 mm
Photon paths configuration	2 full gantry rotations, 90° collimator offset between paths	2 partial 180° - 100° gantry rotations with different gantry-table-collimator paths	2 full gantry rotations, field splitting with 2 cm overlap between paths	2 partial 270°-180° gantry rotations, field splitting with 2 cm overlap between paths
Electron fields/arcs configuration	260° – 230° arcs	1 field 290° gantry angle	280° – 50° arcs	330° – 100° arcs
Robustness analysis parameters				
Random set-up errors sampled from Gaussian distribution, $G(0,\sigma)$, in all directions and combination of them	σ = 4.0 mm	σ = 4.0 mm	σ = 3.0 mm	σ = 7.0 mm
Random as above combined with a systematic 3D translational error	2.0 mm posteriorly, 2.0 mm caudally, 2.0 mm right. Brainstem and optical structures move into the high dose	2.0 mm posteriorly, 2.0 mm caudally, 2.0 mm right. Swallowing and salivary structures move into the high dose	1.5 mm anteriorly, 1.5 mm caudally, 1.5 mm right. Bladder and rectum move into the high dose	3.5 mm anteriorly, 3.5 mm cranially, 3.5 mm right. Heart and lungs move into the high dose

[1]: All plans are normalized to median PTV/CTV for PTV-based and robust optimization respectively.
[2]: The set-up uncertainty magnitude, δ, is derived from the CTV-PTV margin, m, such that $m = 0.7\delta$ (δ rounded). Shifts in each cardinal direction are considered, totaling 7 scenarios (6 with shift + 1 nominal).
[3]: The clinical plan of the head and neck case included a bolus, the PTV was cropped at the skin where there was no bolus. All the plans in this study were without bolus.
Abbreviations: PTV = planning target volume, CTV = clinical target volume, PRV = planning at risk volume.

Results

Figure 2 shows the selected electron energies for the PTV-based and robust-optimized DYMBARC plans with their relative contribution to the target (PTV or CTV) dose after final dose calculation and weight re-optimization for all the cases. Details of the photon and each selected electron beam energies are shown throughout the treated volume in the videos available as supplementary material.

9 Mev electrons with a short range were selected for the head and neck and the breast case, both having targets with very superficial parts. The head and neck target was mostly superficial and 12 MeV were selected as second electron beam energy. However, for the breast case, the target extended deeper and 22 MeV was selected as a second electron beam contributor. These two cases have relatively complicated target shapes with concavities and nodal extension. An important photon contribution was required to cover these irregularities homogeneously. On the other hand, the brain and pelvis case have spheroid/ovoid target shapes that extend from less than a centimeter to more than 7 cm in depth. Here, only rather high electron beam energies of 15-22 MeV were selected that covered most parts of the targets. A smaller photon contribution was used to uniformize coverage and compensate for the shallow electron beam penumbra.

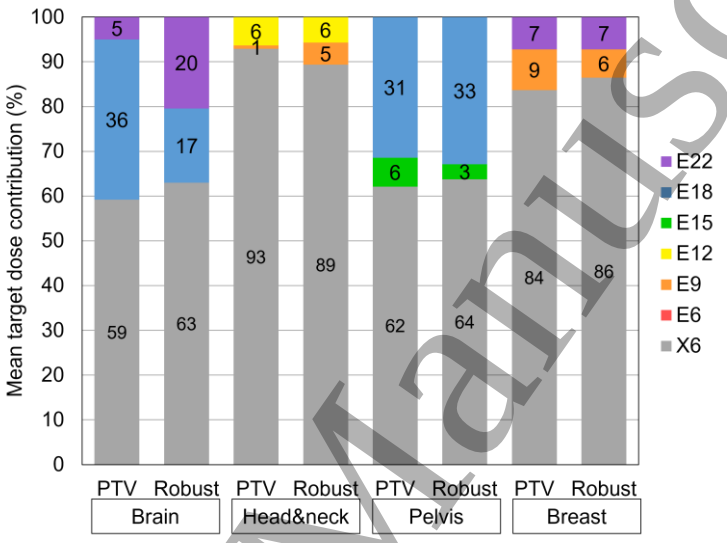

Figure 2. Relative mean target dose contribution for photons and different electron energies in the DYMBARC plans.

DYMBARC plans had lower objective function values than their DTRT counterparts for all cases. For all cases, CTV coverage was similar for all plans in the nominal scenario with variations in D98% and D5% within 1% of the prescription dose.

Table 2: Objective function value after final dose calculation and weight re-optimization for all nominal plans (multiplied by 100).

	PTV-based		Robust-optimized	
	DTRT	DYMBARC	DTRT	DYMBARC
Brain	2.0	1.3	2.2	1.8
Head&neck	2.9	2.7	4.6	4.1
Pelvis	2.4	2.0	2.8	2.2
Breast	4.9	3.4	6.7	5.1

Brain case

Figure 3 shows the DVHs for the nominal (no error) and the error scenarios (see table 1) for all plans. Relevant endpoints are reported in Table 3. CTV D98% deterioration due to set-up uncertainties was the largest for the PTV-based DYMBARC plan where it reached 3% of the prescription dose. Mean dose to the brain was lower in the DYMBARC plans than in the DTRT plans. For serial OARs, near-max doses were higher in the robust-optimized plans compared to the PTV-based plans, where they had a PRV

and the PTV was cropped at its interface for the PTV-based plans. However, near-max dose to serial OAR was more robust for the robust-optimized plans than for PTV-based plans.

Figure 4 shows the dose distribution for both DYMBARC plans in an axial slice where the PTV was cropped at the right optic nerve PRV. The bottom panel shows dose profiles through the white arrow with the 0-position corresponding to the PTV/PRV interface. Relative electron contribution reached >60% of the target coverage along this profile.

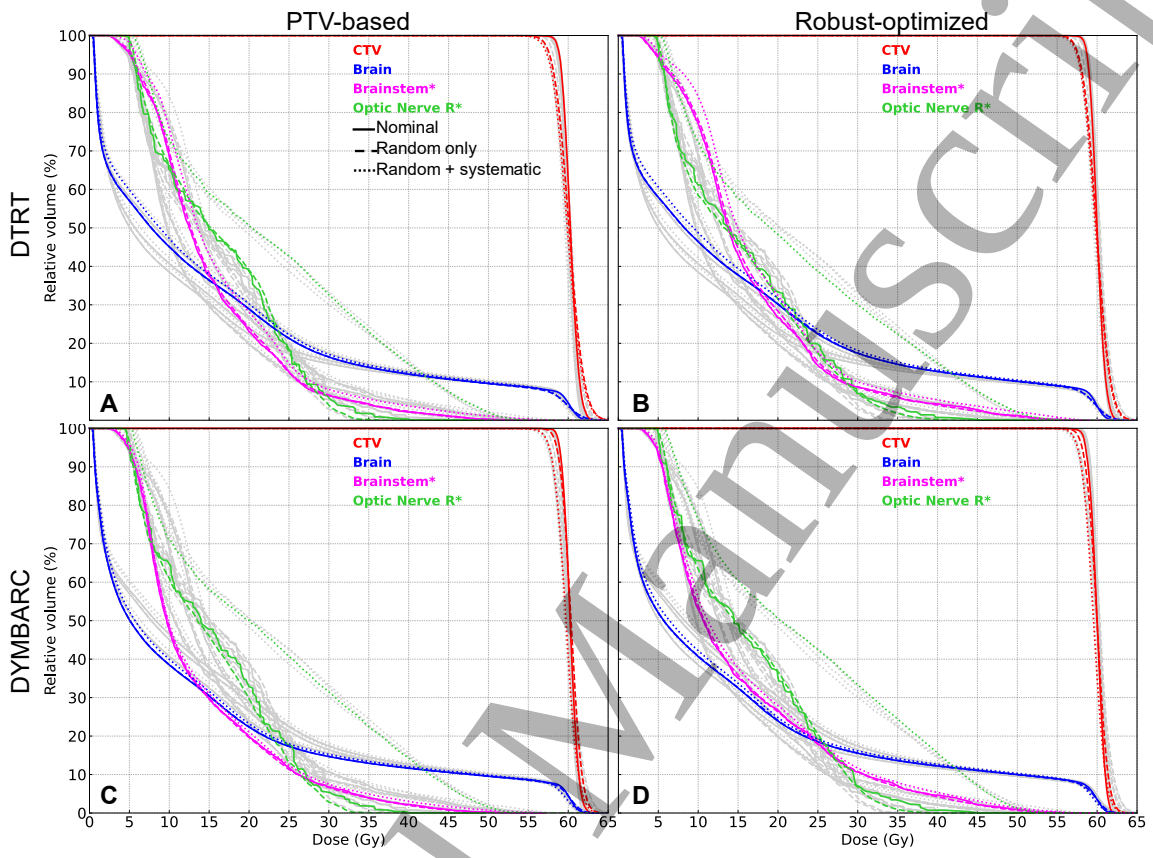

*Figure 3. DVHs for the brain case for the nominal scenario (full line), with random errors (dash line), and with random and systematic errors (dotted line). DVHs are shown in color for the PTV-based DTRT plan in (A), robust-optimized DTRT plan in (B), PTV-based DYMBARC plan in (C), and the robust-optimized DYMBARC plan in (D). All other DVHs are shown in grey for reference. *denotes OARs that have PRV in the PTV-based plan and the PTV is cropped at the PRV interface.*

Table 3. Dosimetric endpoints for the brain case with a 60 Gy prescription dose. *denotes OARs that have PRV in the PTV-based plan and the PTV is cropped at the PRV interface. For each scenario, the best value is shown in bold. ONR = optic nerve right, nom. = nominal, rand. = random, syst. = systematic.

	DTRT PTV-based			DTRT robust-optimized			DYMBARC PTV-based			DYMBARC robust-optimized		
Endpoint [Gy]	nom.	rand.	rand.+ syst.	nom.	rand.	rand.+ syst.	nom.	rand.	rand.+ syst.	nom.	rand.	rand.+ syst.
CTV D98%	58.5	57.0	56.6	58.4	57.0	56.9	**58.6**	**58.1**	**57.0**	58.2	57.6	56.9
CTV D5%	61.8	62.7	62.5	61.4	62.3	62.1	61.6	62.1	61.8	**61.3**	**61.8**	**61.5**
Brain D_{mean}	15.2	15.2	15.8	15.7	15.8	16.4	**13.6**	**13.6**	**14.0**	14.2	14.3	14.7
Brain $D_{2\%}$	60.8	61.0	60.9	**60.5**	60.8	60.8	60.7	60.9	60.5	**60.5**	**60.6**	**60.3**
Brainstem* $D_{2\%}$	**40.7**	41.0	45.9	46.4	46.4	50.6	40.9	**40.0**	**43.6**	45.8	45.5	47.9
ONR* $D_{2\%}$	**33.4**	31.5	50.1	37.5	34.7	50.2	33.8	**31.0**	49.5	37.8	33.3	**49.1**

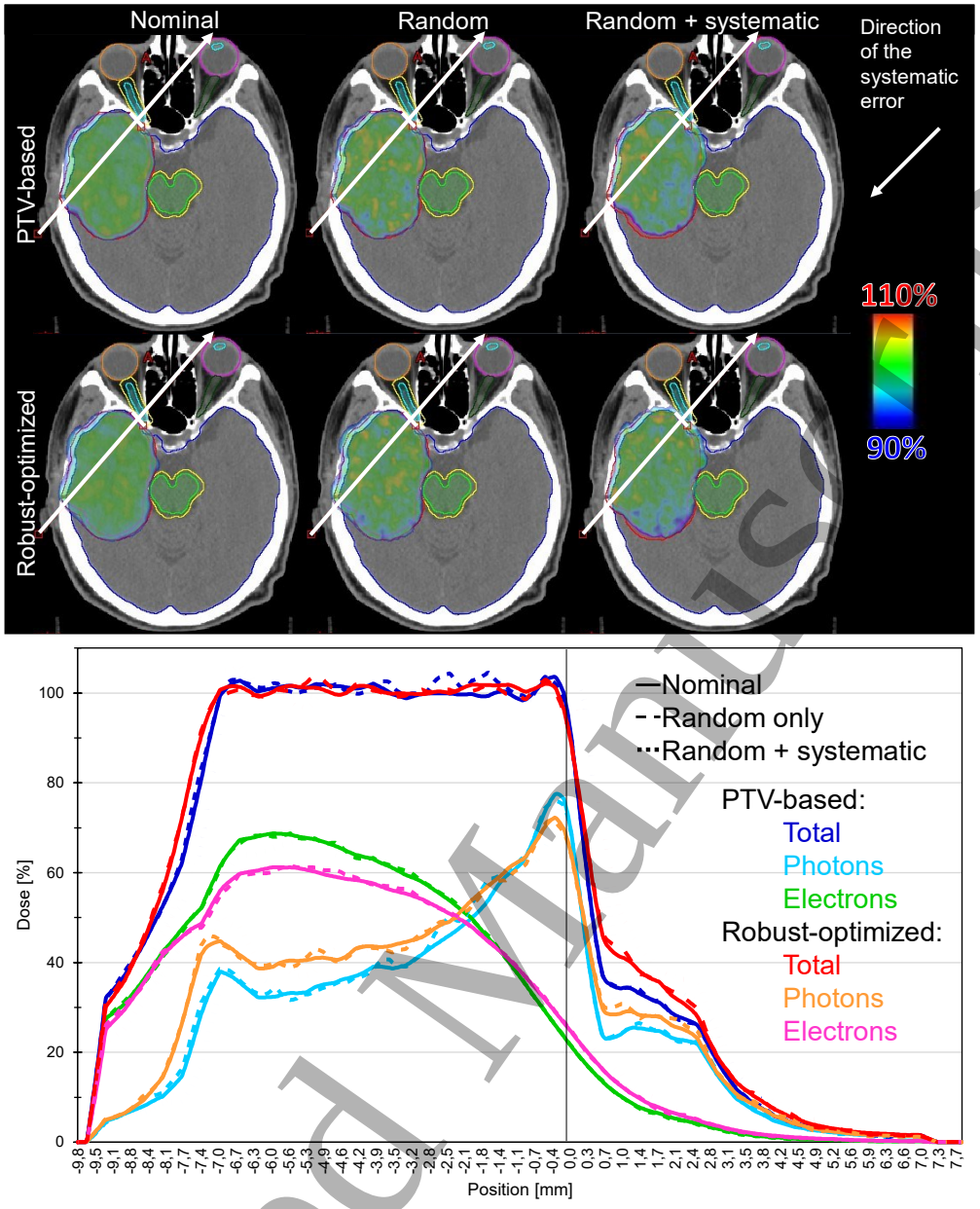

Figure 4: Dose distribution for both DYMBARC plans for the brain case and profiles through the white arrow for the total dose and each particle contribution. Position 0 mm corresponds to the interface between the PTV and the optic nerve PRV.

Head and neck case

Figure 5 shows the DVHs for the nominal and the error scenarios for all plans; relevant endpoints are reported in Table 4. Because the clinical plan included a bolus but not the plans made for this study, the CTV extended very close to the body contour in some places. The PTV was abutting the body contour where the bolus had been removed. Nevertheless, CTV coverage was similar for all plans in the nominal scenario. CTV D98% deterioration in the presence of uncertainties was largest for the PTV-based DTRT plan where it reached 3% of the prescription dose. Mean dose to the ipsilateral submandibular gland, contralateral parotid gland, pharynx, larynx and oral cavity were, on average, lower in the DYMBARC plans compared to the DTRT plans, albeit by small amounts. Large increases in mean dose were observed in the random and systematic error scenario but the robust-optimized plans were more robust than the PTV-based plans.

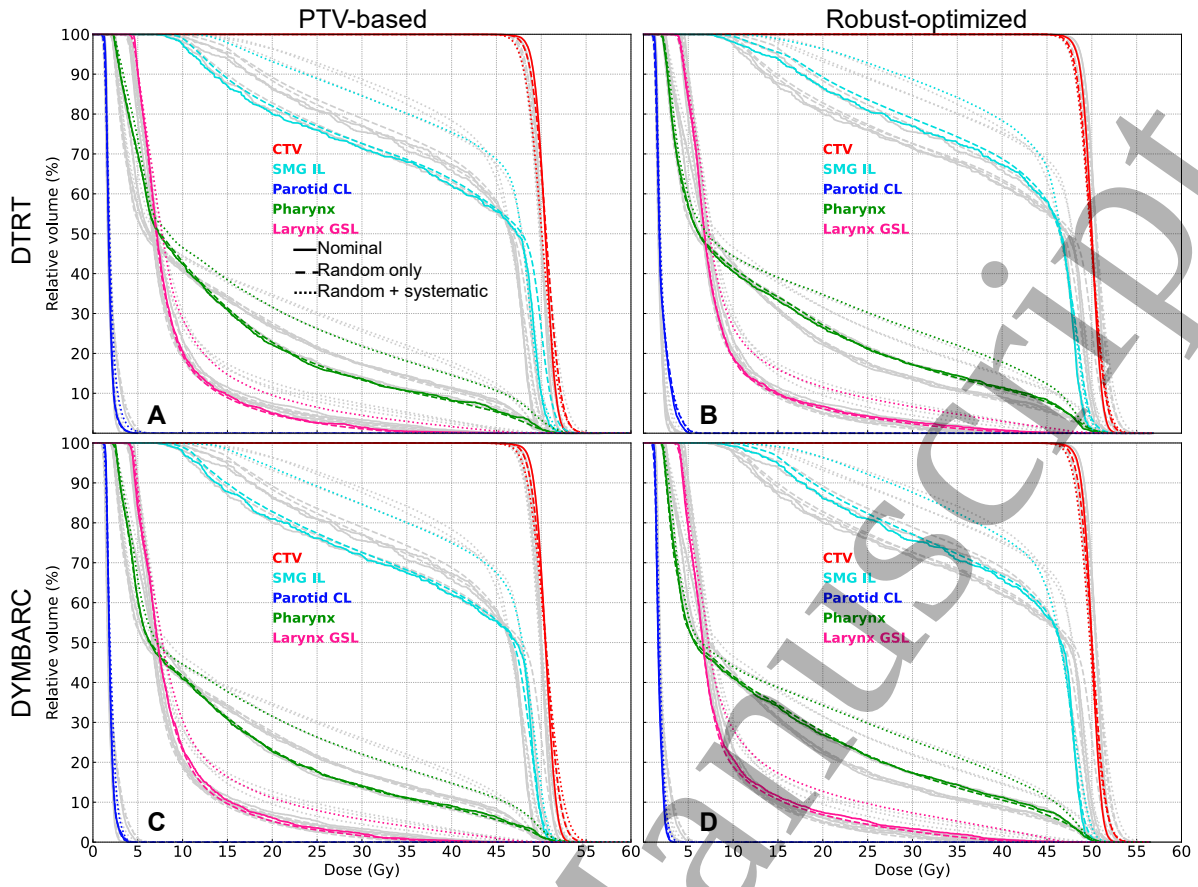

Figure 5: DVHs for the head and neck case for the nominal scenario (full line), with random errors (dash line), and with random and systematic errors (dotted line) for the PTV-based DTRT plan (A), random-optimized DTRT plan (B), PTV-based DYMBARC plan (C).

Table 4. Dosimetric endpoints for the head and neck case with a 50.0Gy prescription dose. For each scenario, the best value is shown in bold. CL: contralateral, IL: ipsilateral, SMG: submandibular gland. nom. = nominal, rand. = random, syst. = systematic.

	DTRT PTV-based			DTRT robust-optimized			DYMBARC PTV-based			DYMBARC robust-optimized		
Endpoint [Gy]	nom.	rand.	rand.+ syst.	nom.	rand.	rand.+ syst.	nom.	rand.	rand.+ syst.	nom.	rand.	rand.+ syst.
CTV D98%	**48.2**	**47.8**	46.9	47.8	47.2	47.0	**48.2**	**47.8**	**47.2**	47.9	47.4	47.0
CTV D5%	52.0	52.7	52.6	**51.4**	**51.9**	52.1	52.0	52.6	53.1	**51.4**	52.0	**52.0**
SMG IL D_{mean}	**38.3**	39.2	42.8	39.5	40.3	43.0	**38.3**	**38.6**	42.8	39.3	39.8	**42.7**
Parotid CL D_{mean}	1.9	1.9	2.0	2.1	2.1	2.2	1.9	2.0	2.0	**1.8**	**1.8**	**1.9**
Pharynx D_{mean}	13.7	13.7	16.8	14.3	14.3	17.1	**13.6**	**13.5**	**16.5**	14.2	14.2	16.8
Larynx D_{mean}	**8.8**	**8.7**	**10.4**	8.9	**8.7**	10.7	9.1	8.9	10.8	9.0	**8.7**	10.9
Oral Cavity D_{mean}	9.8	9.9	11.0	9.8	9.9	11.2	**9.5**	**9.5**	**10.7**	9.6	9.6	10.9

Figure 6 shows the dose distribution for both DYMBARC plans in an axial slice. The bottom panel shows dose profiles through the white arrow with the 0-position corresponding to the PTV/pharynx interface. Relative electron contribution reached >14% (PTV-based) and >20% (robust-optimized) of the target coverage along this profile despite a relative contribution of only 6-11% to the overall target dose.

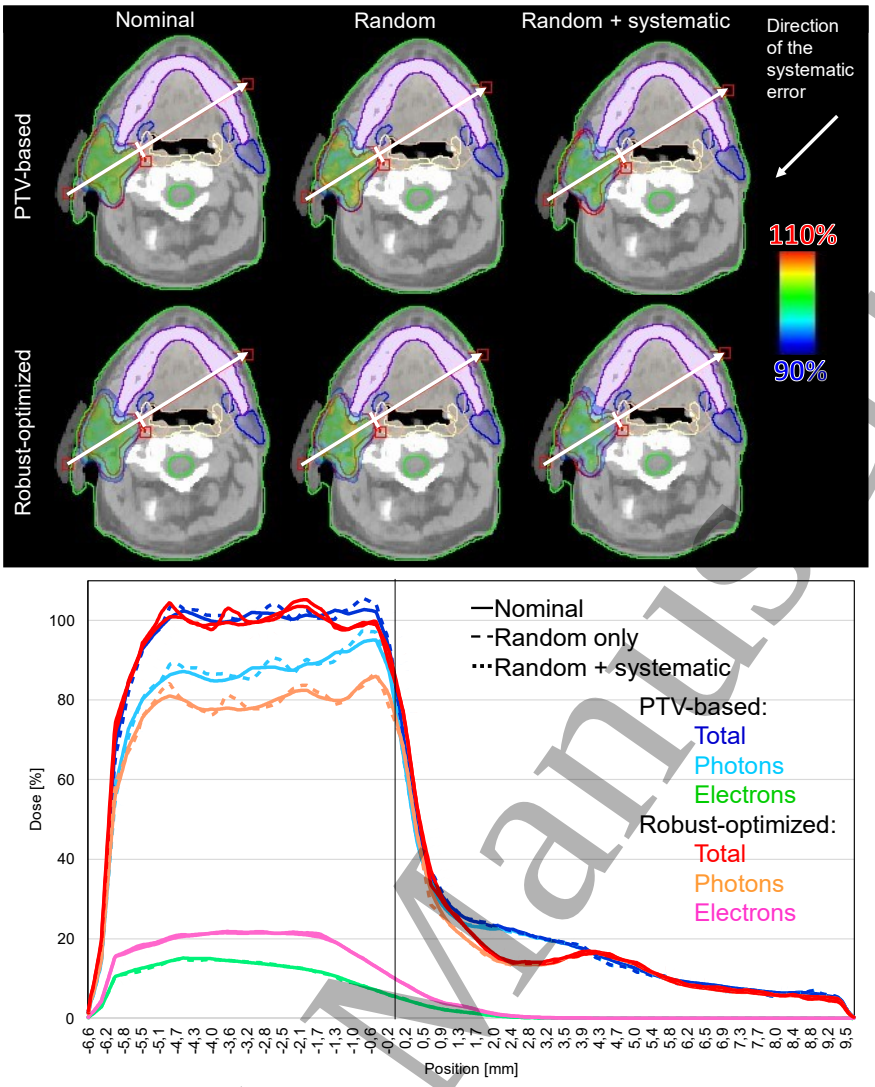

Figure 6: Dose distribution for both DYMBARC plans for the head and neck case and profiles through the white arrow for the total dose and each particle contribution. Position 0 mm corresponds to the interface between the PTV and the pharynx. The clinical plan included a bolus, visible in this image. However, all the plans in this study were without bolus.

Pelvis case

Figure 7 shows the DVHs for the nominal and the error scenarios for all plans; relevant endpoints are reported in Table 5. CTV D98% deterioration in the presence of uncertainties was 2-3% of the prescription dose in all error scenarios. Mean dose to the bladder, rectum, and ipsilateral femoral head was lower for the DYMBARC plans compared to DTRT on average. Figure 8 shows the dose distribution for both DYMBARC plans in an axial slice. The bottom panel shows dose profiles through the white arrow with the 0-position corresponding to the border of the PTV illustrating the high electron contribution to the target dose, especially near the surface.

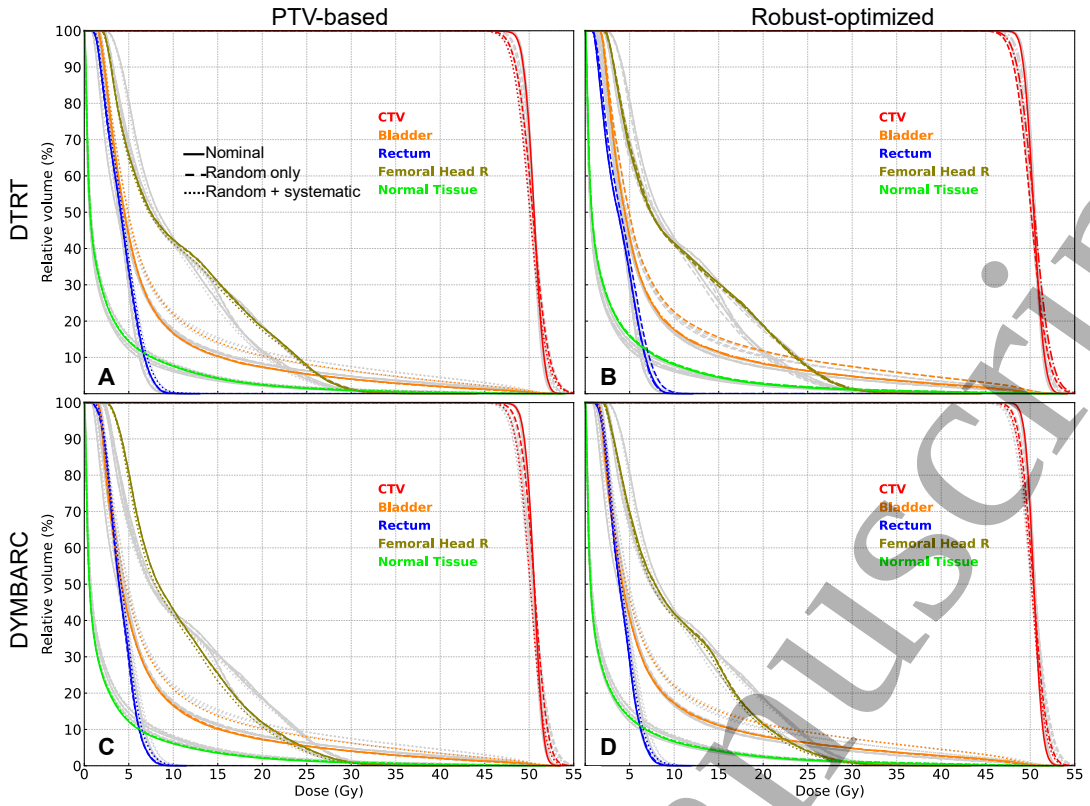

Figure 7: DVHs for the pelvis case for the nominal scenario (full line), with random errors (dash line), and with random and systematic errors (dotted line) for the PTV-based DTRT plan (A), random-optimized DTRT plan (B), PTV-based DYMBARC plan (C), and the robust-optimized DYMBARC plan (D) in color. All other DVHs are shown in grey for reference.

Table 5. Dosimetric endpoints for the Pelvis case with a 50.4 Gy prescription dose. For each scenario, the best value is shown in bold. IL = ipsilateral, nom. = nominal, rand. = random, syst. = systematic.

	DTRT PTV-based			DTRT robust-optimized			DYMBARC PTV-based			DYMBARC robust-optimized		
Endpoint [Gy]	nom.	rand.	rand.+ syst.	nom.	rand.	rand.+ syst.	nom.	rand.	rand.+ syst.	nom.	rand.	rand.+ syst.
CTV D98%	48.6	47.3	47.0	48.6	47.3	47.0	48.7	**47.9**	47.3	**48.8**	47.8	**47.5**
CTV D5%	52.0	52.9	52.6	52.0	53.0	52.6	51.8	52.5	**52.2**	**51.7**	**52.4**	**52.2**
Rectum D_{mean}	4.2	4.2	4.4	**3.9**	**3.9**	**4.3**	4.1	4.1	4.4	4.0	4.0	**4.3**
Bladder D_{mean}	7.4	7.3	8.8	7.7	7.7	9.2	**7.2**	**7.2**	**8.5**	7.5	7.5	8.9
Femoral head IL D_{mean}	11.1	11.0	10.8	11.1	11.1	11.0	10.9	10.9	10.5	**10.5**	**10.5**	**10.2**
Normal tissue D_{mean}	2.7	2.8	2.9	2.9	3.0	3.1	**2.4**	**2.5**	**2.5**	2.6	2.7	2.7

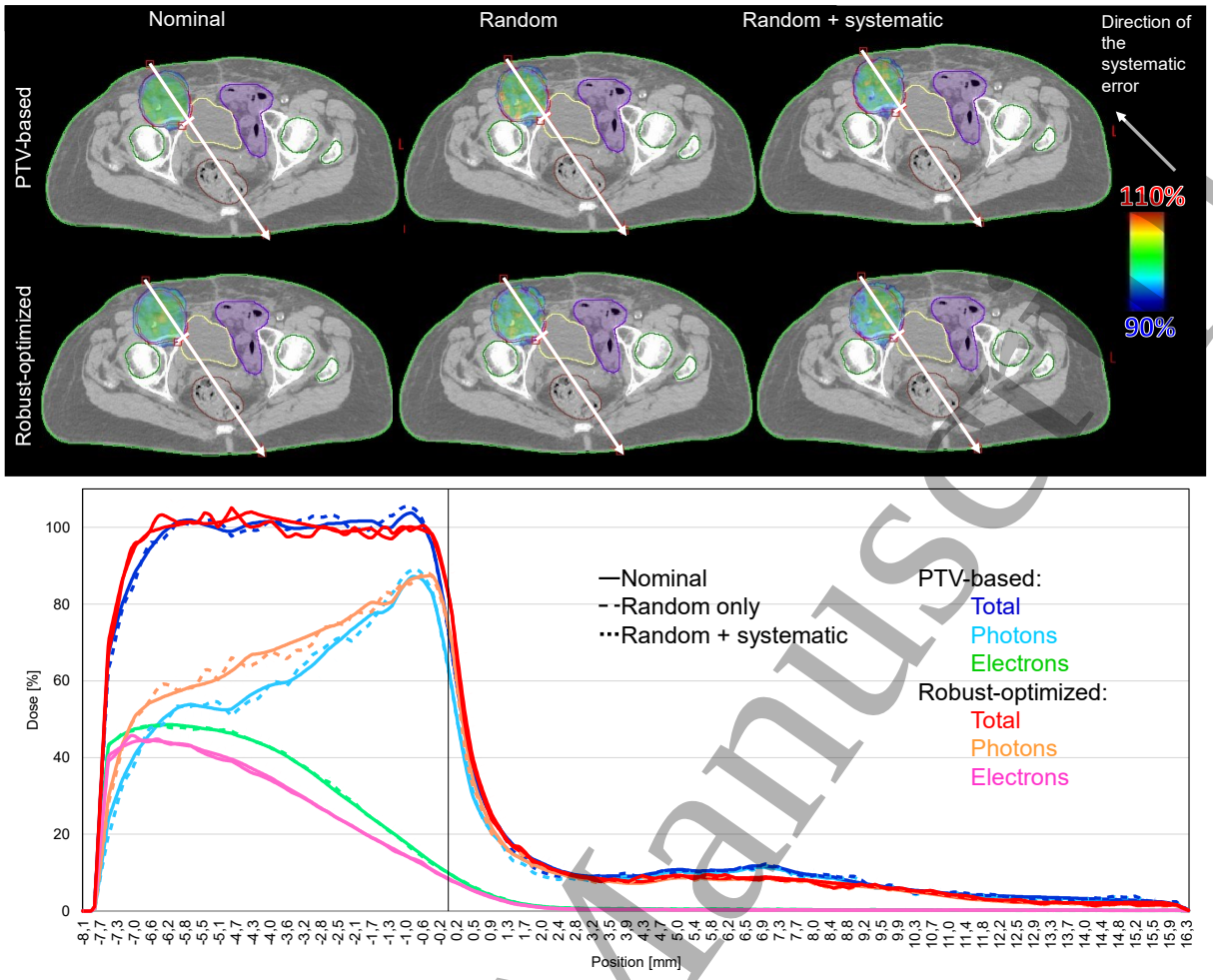

Figure 8: Dose distribution for both DYMBARC plans for the pelvis case and profiles through the white arrow for the total dose and each particle contribution. Position 0 mm corresponds to the border of PTV, in the bladder.

Breast case

Figure 9 shows the DVHs for the nominal and for the error scenarios for all plans; relevant endpoints are reported in Table 6. CTV D98% deterioration in the presence of uncertainties was largest for the PTV-based DYMBARC plan where it reached 4% of the prescription dose. Mean dose to the heart, each lung, and the contralateral breast were lower in the DYMBARC plans compared to the DTRT plans. Mean heart dose was more robust to the combined random and systematic errors for the DYMBARC plans than for the DTRT plans.

Figure 10 shows the dose distribution for both DYMBARC plans in an axial slice. The bottom panel shows dose profiles through the white arrow with the 0-position corresponding to the PTV/chest wall interface. Relative electron contribution reaches >25% of the target coverage along this profile despite a relative contribution of only 13-16% to the overall target dose.

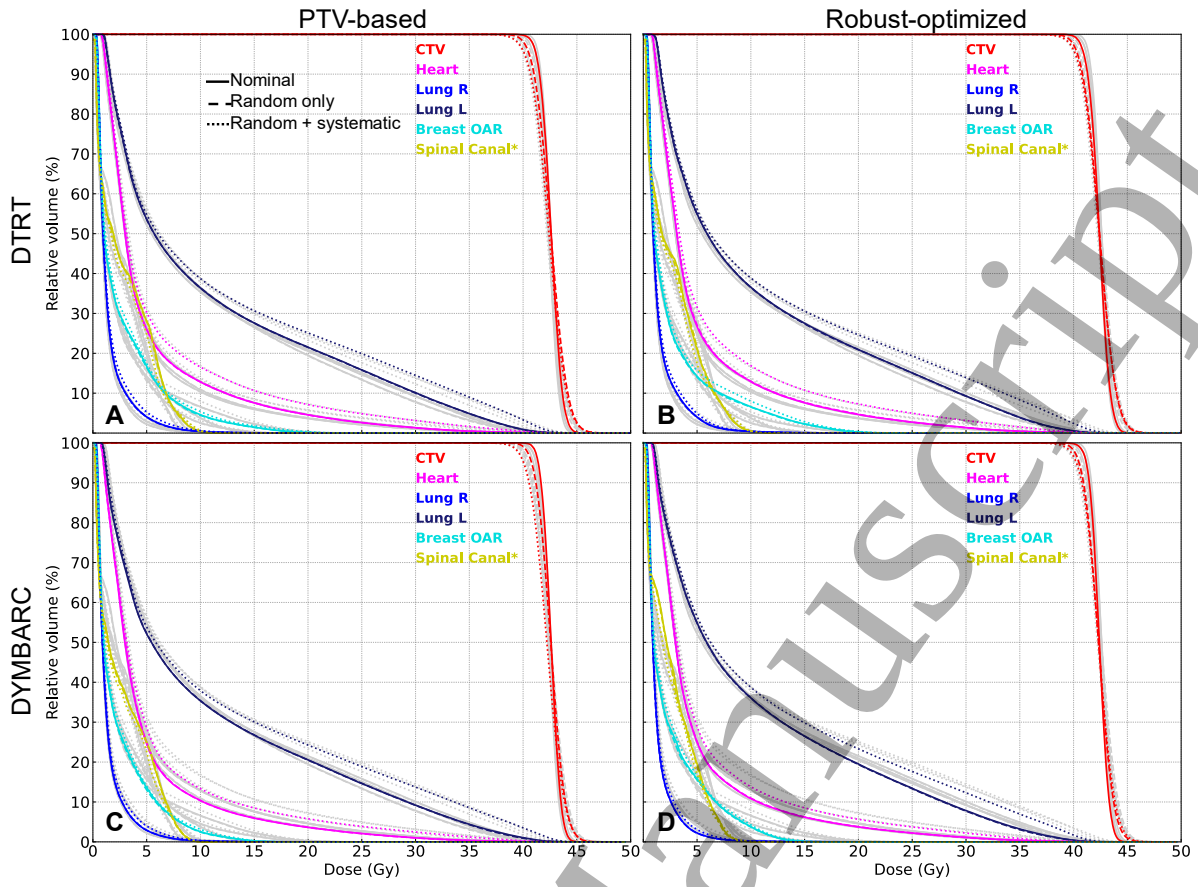

*Figure 9: DVHs for the breast case for the nominal scenario (full line), with random errors (dash line), and with random and systematic errors (dotted line) for the PTV-based DTRT plan (A), random-optimized DTRT plan (B), PTV-based DYMBARC plan (C), and the robust-optimized DYMBARC plan (D) in color. All other DVHs are shown in grey for reference. * denotes OARs that have PRV in the PTV-based plan and the PTV is cropped at the PRV interface.*

Table 6. Dosimetric endpoints for the breast case with a 42.4 Gy prescription dose. For each scenario, the best value is shown in bold. CL = contralateral, IL = ipsilateral, nom. = nominal, rand. = random, syst. = systematic.

	DTRT PTV-based			DTRT robust-optimized			DYMBARC PTV-based			DYMBARC robust-optimized		
Endpoint [Gy]	nom.	rand.	rand.+ syst.	nom.	rand.	rand.+ syst.	nom.	rand.	rand.+ syst.	nom.	rand.	rand.+ syst.
CTV D98%	40.8	40.1	39.5	40.6	39.8	39.5	**41.1**	**40.3**	39.5	40.8	40.0	**39.7**
CTV D5%	44.0	44.6	44.5	**43.7**	44.4	44.5	43.8	44.4	44.3	43.6	**44.1**	**44.3**
Heart D_{mean}	5.2	5.2	6.1	5.3	5.3	6.3	**4.8**	**4.8**	**5.6**	4.9	4.9	**5.6**
CL breast D_{mean}	2.6	2.5	2.8	2.6	2.6	2.8	**2.2**	**2.2**	**2.3**	2.4	2.4	2.5
IL lung D_{mean}	11.0	11.0	12.3	10.9	10.9	12.2	10.6	10.6	12.0	**10.5**	**10.4**	**11.7**
CL Lung D_{mean}	1.4	1.4	1.6	1.4	1.4	1.5	**1.3**	**1.3**	**1.4**	**1.3**	**1.3**	**1.4**

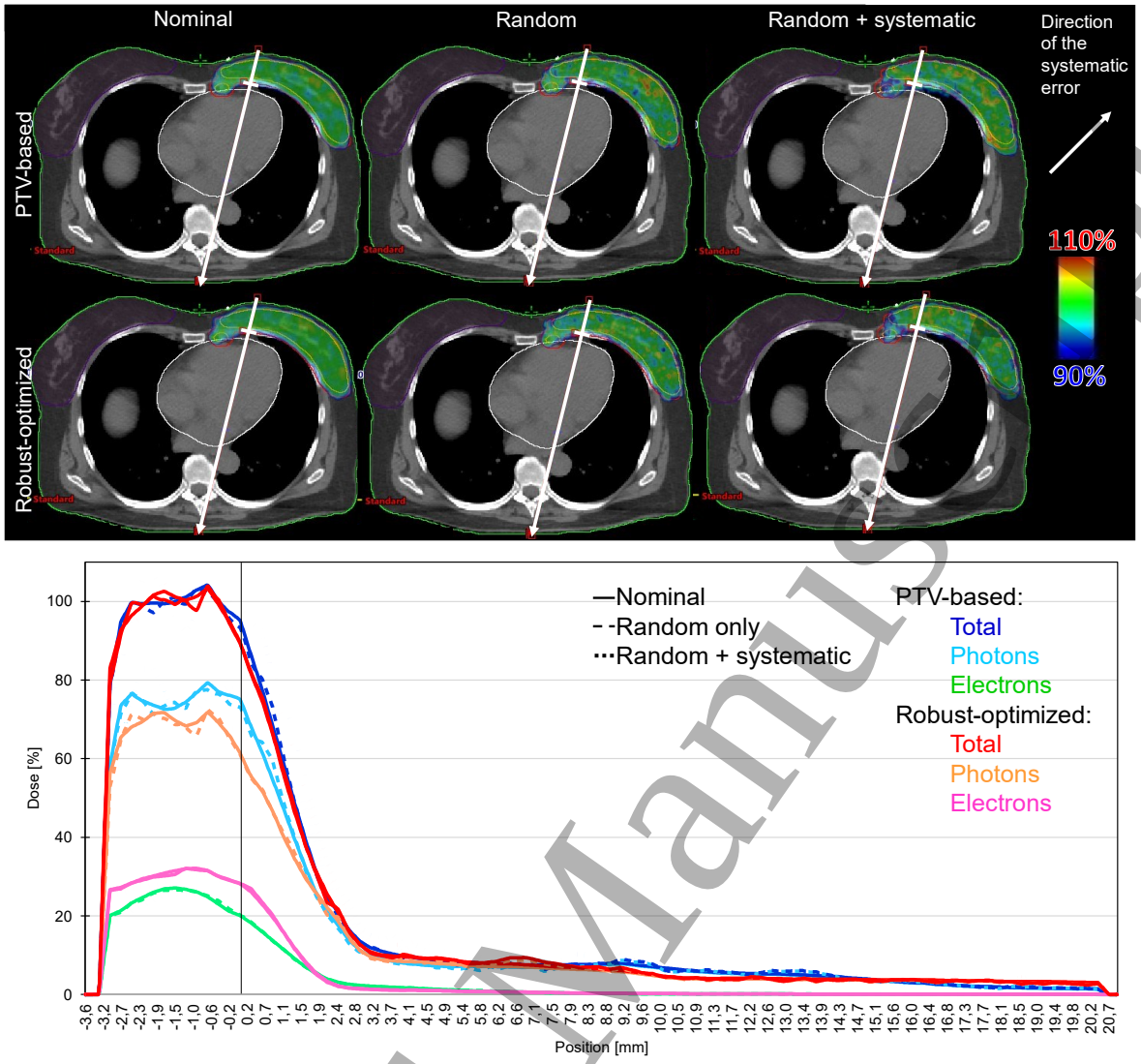

Figure 10: Dose distribution for both DYMBARC plans for the breast case and profiles through the white arrow for the total dose and each particle contribution. Position 0 mm corresponds to the interface between the PTV and the chest wall.

Discussion

This work presents the first use of robust optimization for the novel DTRT and DYMBARC techniques. DYMBARC incorporated non-isocentric coplanar electron arcs with the non-coplanar photon trajectories, resulting in treatment plans that exploit dynamic collimator and gantry rotations, dynamic table rotations (for photon trajectories) and translations (for non-isocentric electron arcs), as well as photon and electron beams of various energies, all with intensity modulation by the MLC on a standard linac. Deliverability with high mechanical and dosimetric accuracy was demonstrated for these types of trajectories in previous studies (Fix *et al* 2018, Mueller *et al* 2018, Bertholet *et al* 2022, Guyer *et al* 2023a, 2022, Manser *et al* 2019). Substituting electron fields for electron arcs in a coplanar geometry was also shown to improve delivery efficiency (Guyer *et al* 2023a). These plans were subject to robustness analysis using a tool that was extensively validated in a previous study (Loebner *et al* 2022).

The addition of electron fields/arcs to the dynamic photon trajectories resulted in a reduction in mean dose to the OARs overall, even for the head and neck and the breast cases where the electrons contributed to less than 20% of the target dose. This was reflected in the objective function values, which were consistently lower for the DYMBARC plans than for the DTRT plans (Table 2). The

improvement in OAR sparing with DYMBARC over DTRT was sometimes small, possibly because the same optimization objectives were used for the two techniques. Optimization objectives could possibly be hardened in the DYMBARC plans to further improve OAR sparing.

For mixed-beam techniques with static fields, Renaud et al (2019) previously observed an increased electron dose contribution in robust plans compared to PTV-based plans. Heath et al (2021) did not observe this effect in their study but identified a trend towards higher electron energies in their robust-optimized plans compared to the PTV-based plans. No clear trend in electron or electron energy contribution was observed in this study. This may be due to the few heterogeneous indications considered, which is a limitation of the study. Our framework should be used to undertake future planning studies to investigate the statistical and clinical significance of these concepts on larger, more homogeneous cohorts. However, although this choice of cases does not permit general conclusions on the impact of using electron fields/arcs or on the use of PTV-based or robust optimization on plan quality, the variety in cases highlights some interesting effects that should be considered when choosing a treatment technique and an optimization strategy and, if applicable, margin manipulation.

The low electron contribution overall for the head and neck and the breast case can be explained by the complexity of the target shape with concavities and nodal extensions (see videos in supplementary material). However, electrons provide most coverage for key superficial target areas, allowing a reduction of healthy tissue dose at depth. For more simple target shapes as in the brain and pelvis cases, more than a third of target coverage is achieved by electrons while the photon contribution is mostly contributing to homogenous dose coverage. Importantly, the photon contribution allows to sharpen the dose gradients at the edge of the target owing to a sharper lateral penumbra than electron beams. This is particularly visible in the brain case (see videos in supplementary material) where the photon dose distribution looks like a “halo” around the distal target edge.

Despite the same electron beam energy selection and arc set-up, relative photon and electron contribution, and especially their spatial dose distribution, varied between PTV-based and robust-based optimization. This was particularly clear for the breast case where the different contributions were more homogeneous in the robust-optimized plan than in the PTV-based plan. The optimizer appears to take advantage of the shallower gradients in the electron dose distributions to improve robustness, especially at target/OAR interfaces. Both the breast (around z = -10 cm) and the head and neck case (around z = -32 cm) had some hot spots for the highest electron beam energy in the PTV-based plan which were not present in the robust-optimized plan (see videos in supplementary material). These observations highlight the unsuitability of the margin concept for intensity modulated electron arcs and support the use of robust optimization for DYMBARC plans.

The brain case had two serial OARs which were extended by a PRV in the PTV-based plan because of their proximity to the CTV. The PTV was cropped at the PRV interface in the PTV-based plans and the near-max dose to these OARs was lower in the PTV-based plans than in the robust-optimized plans for both DTRT and DYMBARC. However, a systematic error pushing these OARs into the high dose region resulted in an increase in near-max dose for all plans but reduced or even, for the optic nerve, inverted the difference between PTV-based and robust-optimized plans. Degradation in CTV coverage was also higher in the PTV-based plans compared to the robust plans, likely due to the PTV cropping. This highlights the limitation of the margin concepts when targets abut serial OARs. Robust optimization appears to handle conflicting objectives more effectively.

In the head and neck case, parallel OARs are overlapping with the target volume. Electron contribution was low in the DYMBARC plans and the differences in OAR sparing between DTRT and DYMBARC were also low. However, there were marked differences between PTV-based and robust optimization for this

case. The PTV-based plans had better pharynx and ipsilateral submandibular gland sparing than the robust-optimized plans; however, they were also more affected by random and systematic uncertainties. Similarly to the case of OARs abutting CTVs like in the brain case, robust optimization appears to handle conflicting objectives more effectively than PTV-based optimization when parallel OARs overlap with the CTV.

Furthermore, the head and neck case had a bolus, but the plans created in this study were without bolus and resulted in good CTV coverage with CTV D98% above 95% of the prescription dose. Adequate coverage, despite the removal of the bolus, could be expected for the DYMBARC plans owing to the higher entrance dose for electron compared to photon fields; nevertheless, CTV coverage was equally high in the DTRT plans in the nominal scenario. This could be the result of the non-coplanar geometry where high surface dose can be achieved through the use of multiple tangential beam directions. In the random and systematic error scenario however, CTV coverage was most affected in the PTV-based DTRT plan (figure 5). In a study of robust optimized mixed-beam RT for soft tissue sarcoma, Heng et al (2023) also reported that bolus could be omitted for superficial targets. Together with our results, this indicates that mixed-beam techniques and/or non-coplanar beam directions may negate the need for bolus in superficial targets but robust optimization is needed to ensure coverage under set-up uncertainties.

The pelvis case had the second highest electron contribution in the DYMBARC plans but this resulted in relatively small improvement in OAR sparing (0.4% of the prescription dose on average for the mean dose to the rectum, bladder and ipsilateral femoral head). Nevertheless, the normal tissue dose was consistently lower at all dose levels for the DYMBARC plans compared to the DTRT plans (Figure 7). CTV coverage was also more robust in the DYMBARC plans than in the DTRT plans.

For the breast case, all OARs were better spared in the DYMBARC plans compared to the DTRT plans despite an electron contribution of only 13-16% of the target dose. Guyer et al (2023a) also observed a general reduction in OAR dose for mixed-beam plans compared to photon-only plans for four breast cancer cases. In the present study, mean heart dose was also less affected by random and systematic errors in the DYMBARC plans than in the DTRT plans. These results further support the use of electron arcs for breast cancer treatments to improve both OAR sparing and robustness to set-up uncertainties. However, CTV coverage was most affected in the PTV-based DYMBARC plan, which may be due to the fundamental issues of margin definition in electron therapy (Thomas 2006) and/or the PTV cropping at the skin. Robust optimization was also shown to be superior to PTV-based planning for VMAT breast treatments (Liang *et al* 2020, Dunlop *et al* 2019). Further investigations of robust-optimized mixed-beam plans (arc-MBRT or DYMBARC) should be conducted to confirm the benefit of mixed-beam techniques for breast cancer treatments and clarify the potential need for robust optimization.

Interestingly, with the exception of the breast case, the addition of electron arcs/fields to the photon paths appeared to improve robustness also for the PTV-based plans. This was not expected given the fundamental limitations of the margin concept for electron fields. This may indicate that, the effect of uncertainties on the dose distribution are smoothed out or compensated by the combination of photons and electrons to a certain extent.

Most studies comparing PTV-based to robust optimization consider the same scenarios for robust optimization and robust analysis, generally for uncertainty scenarios of 5 mm in each cardinal direction, regardless of the CTV-PTV margin used in the PTV-based plans (Heath *et al* 2021, Renaud *et al* 2019, Heng *et al* 2023). Robustness tends to be evaluated on the same uncertainties as those used for robust optimization. In the present study, different cases with CTV-PTV margins between 2 and 7 mm were considered and the magnitude of the uncertainty scenarios considered for robust

optimization were derived from the margin so both concepts are designed to address uncertainties of similar magnitude. This design should be considered in future planning studies. Whereas robust optimization considered uncertainties in each cardinal direction, the robustness analysis considered more complex and more realistic error scenarios with random set-up errors sampled from a gaussian distribution, also including combination of errors in multiple directions. An additional systematic error was investigated, in the 3D direction that pushes the nearby OARs into the high dose region. This systematic error was the most favorable in terms of target coverage for certain cases, notably the head and neck cases with the PTV cropped on the opposite direction. However, the purpose was to explore a potential worst-case scenario in terms of OAR sparing. Although more scenarios could be included in the robust optimization, this would considerably increase beamlet dose calculation and plan optimization times. Yet, our study shows that robust optimization based on the nominal scenario plus six simple uncertainty scenarios can already generate plans that remain robust to more complex error scenarios. Robust-optimization remained favorable compared to PTV-based optimization in this stringent assessment. A previous robustness assessment study has shown that the margin concept was suitable for DTRT for a large head and neck cohort (Loebner *et al* 2024). With this study, we bring DYMBARC closer to clinical applicability by providing a solution to the limitations of the margin concept for mixed-beam techniques and show that robust optimization may also outperform the margin concept for DTRT.

Finally, this study highlights the versatility of our in-house optimizer and robustness analysis tools. Simultaneous optimization of photon and electron contributions for dynamic paths, arcs, or fields using the same types of optimization objectives permits direct technique comparison based on the objective function value for different techniques. Electron energy selection is based on dosimetric quality during an intermediate DAO step. Two energies were selected in this study based on the results of Guyer et al (2023a) showing that adding more electron energies did not improve dosimetric plan quality but increased estimated delivery time. Both PTV-based and robust optimization are available and additional uncertainty scenarios can be included in the optimization as well as in the robustness analysis. The interface between the in-house software and research version of Eclipse enables smooth paths, arcs, and fields set-up, beamlet dose calculation, and plan evaluation and comparison, based on CT images and contours as they are used for clinical treatment planning. Hence, plans can be compared for different techniques (DTRT vs DYMBARC) and optimization strategy (PTV vs robust optimization) using the same environment.

Conclusions

This study introduced robust optimization for DTRT and DYMBARC, a modality incorporating non-isocentric coplanar electron arcs with the dynamic non-coplanar photon trajectories. For a small but diverse cohort, robust-optimized plans were more robust to random and systematic uncertainties compared to PTV-based plans; this was especially true when PTV margins had been manipulated or when OARs were abutting or overlapping with the target. DYMBARC plans were generally more robust than DTRT plans; specifically, electron profiles were less affected by systematic errors compared to photon profiles. DYMBARC plans had similar target coverage but better OAR sparing than DTRT plans.

Acknowledgements

This work was supported by grant 200021_185366 of the Swiss National Science Foundation and by Varian, a Siemens Healthineers Company. Calculations were performed on UBELIX (http://www.id.unibe.ch/hpc), the HPC cluster at the University of Bern.

References

Bertholet J, Mackeprang P-H, Mueller S, Guyer G, Loebner H A, Wyss Y, Frei D, Volken W, Elicin O, Aebersold D M, Fix M K and Manser P 2022 Organ-at-risk sparing with dynamic trajectory radiotherapy for head and neck cancer: comparison with volumetric arc therapy on a publicly available library of cases *Radiation Oncology* **17** 122 Online: https://ro-journal.biomedcentral.com/articles/10.1186/s13014-022-02092-5

Dunlop A, Colgan R, Kirby A, Ranger A and Blasiak-Wal I 2019 Evaluation of organ motion-based robust optimisation for VMAT planning for breast and internal mammary chain radiotherapy *Clin Transl Radiat Oncol* **16** 60–6

Fix M K, Cygler J, Frei D, Volken W, Neuenschwander H, Born E J and Manser P 2013 Generalized eMC implementation for Monte Carlo dose calculation of electron beams from different machine types *Phys Med Biol* **58** 2841–59

Fix M K, Frei D, Mueller S, Guyer G, Loebner H A, Volken W and Manser P 2023 Auto-commissioning of a Monte Carlo electron beam model with application to photon MLC shaped electron fields *Phys Med Biol* **68** 044004

Fix M K, Frei D, Volken W, Terribilini D, Mueller S, Elicin O, Hemmatazad H, Aebersold D M and Manser P 2018 Part 1: Optimization and evaluation of dynamic trajectory radiotherapy *Med Phys* **45** 4201–12

Fix M K, Manser P, Frei D, Volken W, Mini R and Born E J 2007 An efficient framework for photon Monte Carlo treatment planning *Phys Med Biol* **52**

Guyer G, Mueller S, Koechli C, Frei D, Volken W, Bertholet J, Mackeprang P-H, Loebner H A, Aebersold D M, Manser P and Fix M K 2022 Enabling non-isocentric dynamic trajectory radiotherapy by integration of dynamic table translations *Phys Med Biol* **67** 175003 Online: https://iopscience.iop.org/article/10.1088/1361-6560/ac840d

Guyer G, Mueller S, Mackeprang P-H, Frei D, Volken W, Aebersold D M, Loessl K, Manser P and Fix M K 2023a Delivery time reduction for mixed photon-electron radiotherapy by using photon MLC collimated electron arcs *Phys Med Biol* **68** 215009 Online: https://iopscience.iop.org/article/10.1088/1361-6560/ad021a

Guyer G, Mueller S, Wyss Y, Bertholet J, Schmid R, Stampanoni M F M, Manser P and Fix M K 2023b Technical note: A collision prediction tool using Blender *J Appl Clin Med Phys* Online: https://aapm.onlinelibrary.wiley.com/doi/10.1002/acm2.14165

Heath E, Mueller S, Guyer G, Duetschler A, Elicin O, Aebersold D, Fix M K and Manser P 2021 Implementation and experimental validation of a robust hybrid direct aperture optimization approach for mixed-beam radiotherapy *Med Phys* **48** 7299–312

Heng V J, Serban M, Renaud M A, Freeman C and Seuntjens J 2023 Robust mixed electron-photon radiation therapy planning for soft tissue sarcoma *Med Phys* **50** 6502–13

Henzen D, Manser P, Frei D, Volken W, Neuenschwander H, Born E J, Vetterli D, Chatelain C, Stampanoni M F M and Fix M K 2014 Monte Carlo based beam model using a photon MLC for modulated electron radiotherapy *Med Phys* **41** 021714

van Herk M 2004 Errors and margins in radiotherapy. *Semin Radiat Oncol* **14** 52–64

Hernandez V, Hansen C R, Widesott L, Bäck A, Canters R, Fusella M, Götstedt J, Jurado-Bruggeman D, Mukumoto N, Kaplan L P, Koniarová I, Piotrowski T, Placidi L, Vaniqui A and Jornet N 2020 What is plan quality in radiotherapy? The importance of evaluating dose metrics, complexity, and robustness of treatment plans *Radiotherapy and Oncology* **153** 26–33 Online: https://linkinghub.elsevier.com/retrieve/pii/S0167814020308136

Kawrakow I and Fippel M 2000 VMC++, a fast MC algorithm for Radiation Treatment planning *The Use of Computers in Radiation Therapy* (Berlin, Heidelberg: Springer Berlin Heidelberg) pp 126–8

Korevaar E W, Habraken S J M, Scandurra D, Kierkels R G J, Unipan M, Eenink M G C, Steenbakkers R J H M, Peeters S G, Zindler J D, Hoogeman M and Langendijk J A 2019 Practical robustness evaluation in radiotherapy – A photon and proton-proof alternative to PTV-based plan evaluation *Radiotherapy and Oncology* **141** 267–74

Langhans M, Unkelbach J, Bortfeld T and Craft D 2018 Optimizing highly noncoplanar VMAT trajectories: The NoVo method *Phys Med Biol* **63**

Liang X, Bradley J A, Mailhot Vega R B, Rutenberg M, Zheng D, Getman N, Norton K W, Mendenhall N and Li Z 2020 Using Robust Optimization for Skin Flashing in Intensity Modulated Radiation Therapy for Breast Cancer Treatment: A Feasibility Study *Pract Radiat Oncol* **10** 59–69

Loebner H A, Bertholet J, Mackeprang P-H, Volken W, Elicin O, Mueller S, Guyer G, Aebersold D M, Stampanoni M F M, Fix M K and Manser P 2024 Robustness analysis of dynamic trajectory radiotherapy and volumetric modulated arc therapy plans for head and neck cancer *Phys Imaging Radiat Oncol* 100586

Loebner H A, Volken W, Mueller S, Bertholet J, Mackeprang P, Guyer G, Aebersold D M, Stampanoni M F M, Manser P and Fix M K 2022 Development of a Monte Carlo based robustness calculation and evaluation tool *Med Phys* Online: https://onlinelibrary.wiley.com/doi/10.1002/mp.15683

Manser P, Frauchiger D, Frei D, Volken W, Terribilini D and Fix M K 2019 Dose calculation of dynamic trajectory radiotherapy using Monte Carlo *Z Med Phys* **29** 31–8 Online: https://doi.org/10.1016/j.zemedi.2018.03.002

Mueller S, Guyer G, Risse T, Tessarini S, Aebersold D M, Stampanoni M F M, Fix M K and Manser P 2022 A hybrid column generation and simulated annealing algorithm for direct aperture optimization *Phys Med Biol* **67** 075003 Online: https://iopscience.iop.org/article/10.1088/1361-6560/ac58db

Mueller S, Guyer G, Volken W, Frei D, Torelli N, Aebersold D M, Manser P and Fix M K 2023 Efficiency enhancements of a Monte Carlo beamlet based treatment planning process: implementation and parameter study *Phys Med Biol* **68**

Mueller S, Manser P, Volken W, Frei D, Kueng R, Herrmann E, Elicin O, Aebersold D M, Stampanoni M F M and Fix M K 2018 Part 2: Dynamic mixed beam radiotherapy (DYMBER): Photon dynamic trajectories combined with modulated electron beams *Med Phys* **45** 4213–26

Neuenschwander H, Mackie T R and Reckwerdt P J 1995 MMC-a high-performance Monte Carlo code for electron beam treatment planning *Phys Med Biol* **40** 543–74

Renaud M A, Serban M and Seuntjens J 2019 Robust mixed electron–photon radiation therapy optimization *Med Phys* **46** 1384–96

Smyth G, Bamber J C, Evans P M and Bedford J L 2013 Trajectory optimization for dynamic couch rotation during volumetric modulated arc radiotherapy *Phys Med Biol* **58** 8163–77

Stroom J C, De Boer H C J, Huizenga H and Visser A G 1999 Inclusion of geometrical uncertainties in radiotherapy treatment planning by means of coverage probability *Int J Radiat Oncol Biol Phys* **43** 905–19

Stroom J C and Heijmen B J M 2002 Geometrical uncertainties, radiotherapy planning margins, and the ICRU-62 report *Radiotherapy and Oncology* **64** 75–83

Thomas S J 2006 Margins between clinical target volume and planning target volume for electron beam therapy *Br J Radiol* **79** 244–7

Unkelbach J, Alber M, Bangert M, Bokrantz R, Chan T C Y, Deasy J O, Fredriksson A, Gorissen B L, Van Herk M, Liu W, Mahmoudzadeh H, Nohadani O, Siebers J V., Witte M and Xu H 2018 Robust radiotherapy planning *Phys Med Biol* **63**

Yang Y, Zhang P, Happersett L, Xiong J, Yang J, Chan M, Beal K, Mageras G and Hunt M 2011 Choreographing couch and collimator in volumetric modulated arc therapy *Int J Radiat Oncol Biol Phys* **80** 1238–47